Vortex matter stabilized by many-body interactions

S. Wolf,[1,2,3] A. Vagov,[1] A. A. Shanenko,[4] V. M. Axt,[1] and J. Albino Aguiar[4]
[1]*Institut für Theoretische Physik III, Bayreuth Universität, Bayreuth 95440, Germany*
[2]*Institut für Theoretische Physik, Technische Universität Dresden, Dresden 01062, Germany*
[3]*School of Physics, University of Melbourne, Parkville, VIC 3010, Australia*
[4]*Departamento de Física, Universidade Federal de Pernambuco, Av. Jorn. Aníbal Fernandes, s/n, Cidade Universitária 50740-560, Recife, PE, Brazil*
(Received 22 June 2017; revised manuscript received 17 October 2017; published 30 October 2017)

This work investigates interactions of vortices in superconducting materials between standard types I and II, in the domain of the so-called intertype (IT) superconductivity. Contrary to common expectations, the many-body (many-vortex) contribution is not a correction to the pair-vortex interaction here but plays a crucial role in the formation of the IT vortex matter. In particular, the many-body interactions stabilize vortex clusters that otherwise could not exist. Furthermore, clusters with large numbers of vortices become more stable when approaching the boundary between the intertype domain and type I. This indicates that IT superconductors develop a peculiar unconventional type of the vortex matter governed by the many-body interactions of vortices.

DOI: 10.1103/PhysRevB.96.144515

I. INTRODUCTION

It is well known that the textbook classification of the superconductivity types [1–3] does not apply for materials with the Ginzburg-Landau (GL) parameter close to the critical value $\kappa \sim \kappa_0$ ($\kappa_0 = 1/\sqrt{2}$) [4–18]. Such materials, that can be broadly referred to as intertype (IT) superconductors, demonstrate properties that cannot be described within the type I/II dichotomy. Experimentally, the IT regime reveals itself most obviously in a first-order transition between the Meissner and mixed states, seen as an abrupt change (drop) in the magnetization [4–13,17]. This discontinuity has been observed in Ta (under doping by nitrogen), Nb (clean and doped by nitrogen), V, $LaAl_2$, and in alloys Pb-Tl, Pb-In, and In-Bi [4–6,8,11]. Recently the same transition has also been reported for ZrB_{12} [19–21].

The IT superconductivity regime can also be achieved by varying geometry of a sample. For example, this can be done for superconducting films made of a type I material (e.g., Pb, Sn, or In) and placed in a perpendicular magnetic field. When the film thickness decreases, superconductivity of type I is replaced by that of type II [22–24], passing through the IT regime [25–27]. A similar geometry induced type-II behavior has been recently observed for arrays of superconducting wires made of β-gallium [28].

In conventional single-band superconductors the interval of κ, which corresponds to the IT regime, is rather narrow (see, e.g., Refs. [8,11]). However, in multiband superconductors the IT domain in the (κ, T) plain has been predicted to widen notably [29]. For example, a large IT domain can be expected in so-called BCS-BEC superconductors, where the BEC condensates of shallow bands coexist with the BCS condensates of standard deep bands [30]. Evidences of the BCS-BEC superconductivity and the related BCS-BEC crossover have been recently reported for iron chalcogenides FeSe and $FeSe_xTe_{1-x}$ [31–33]. Consequently, multiband superconductors appear to considerably expand the class of IT materials.

Magnetic properties of superconductors are closely related with the mechanism of how the magnetic field penetrates a superconductor. Therefore, details of this mechanism have a direct influence on fundamental superconducting characteristics such as, e.g., the critical magnetic fields and the critical current.

Most of experimental evidences suggest that the magnetic field penetrates IT superconductors in the form of Abrikosov (single-quantum) vortices [4–6,8,14–16,18]. Until recently it was assumed that the defining feature of the IT regime is a spatially nonmonotonic vortex interaction [4–18]. Following this view, Abrikosov vortices play a role of elementary "particles" of the mixed state in both IT and type-II superconductors while their relatively weak interaction helps to arrange them in a particular form of the Abrikosov lattice. Within this picture all differences between IT and type II superconductors are explained only in terms of the vortex interaction: it is attractive at long ranges in the IT regime while fully repulsive in type II. Acknowledging this similarity, the name "type II/1" was coined for IT superconductors [8,17] while type II was denoted as "type II/2". It was believed that the vortex interaction in IT superconductors is essentially of the two-body character, i.e., the same as in type II, while the many-body (many-vortex) interactions can contribute only in condensates with multiple competing order parameters [34–37].

This concept of the IT superconductivity has been challenged in recent studies [29,30,38] that connected the physics in the IT domain with the self-duality of the GL theory at κ_0 [39,40] and the related infinite degeneracy of the condensate state in the Bogomolnyi point (κ_0, T_c) (T_c is the critical temperature). This point separates types I and II at $T = T_c$, while at $T < T_c$ the degeneracy is removed and the Bogomolnyi point unfolds into a finite IT domain in the (κ, T) plane with a variety of unconventional properties. The degeneracy can also be removed by other factors, e.g., by the contribution of stray fields in finite samples [38].

It has been demonstrated [29] that the nonmonotonic vortex interaction is only one example of the unconventional properties in the mixed state of IT superconductors. Its appearance determines the upper boundary of the IT domain [8,11,29]. Other nonstandard properties, e.g., stable isolated multiquantum vortices [29], emerge sequentially when the

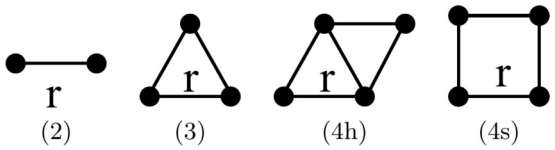

FIG. 1. Considered vortex configurations; solid circles denote positions of vortices and r is the distance between the nearest neighbors.

system "moves" across the IT domain to its lower boundary, where the mixed state finally disappears [8,11,29]. Recent theoretical studies have shown that the IT regime in superconducting films reveals itself via a manifold of highly unusual spatial condensate-field patterns [38].

The findings of Refs. [29,30,38] paint a much more complex picture than that of the type II/1,2 concept. In particular, the view on Abrikosov vortices as elementary "particles" of the mixed state is questioned by the observation [29] that isolated vortices (both single and multiquantum) are unstable in a large part of the IT domain referred to as IT/I (the subdomain with stable isolated vortices is referred to as IT/II). This raises a question of whether the mixed state in the IT/I regime can still be formed by vortices or the mixed state has a totally different nature here. The vortex matter can still appear if stabilized by the vortex interaction.

In this work we show that contrary to common expectations, vortex interactions in the IT/I subdomain are essentially of the many-body character. Furthermore, the number of vortices contributing to the many-body interactions increases in superconductors that are closer to type I. In this case the many-body interactions stabilize the vortex matter which otherwise could not exist. It is, therefore, demonstrated that the mixed state in the IT/I subdomain differs qualitatively from that in type-II and IT/II, representing an atypical vortex matter, where vortices cannot be considered as weakly two-body interacting.

II. FORMALISM

A many-body component of the vortex interaction is evaluated for N-vortex clusters with $N = 2$, 3, and 4 (see Fig. 1). We take the 3-vortex cluster in the form of an equilateral triangle, while for 4-vortex clusters we consider the rhombic or hexagonal h-configuration (a part of the hexagonal lattice) and also the square s configuration. The vortex interaction potential can be extracted from the free energy of the superconducting condensate with the chosen positions of the vortex centers, from which the energy of isolated (infinitely separated) vortices is subtracted.

In practical calculations it is more convenient to work with the Gibbs free energy G with the density $g = f - (\mathbf{H}\cdot\mathbf{B})/4\pi$, where $\mathbf{B}$ is the magnetic field (induction) and $\mathbf{H}$ is the external (uniform) field, both directed along the z axis. One notes that the volume integral of $(\mathbf{H}\cdot\mathbf{B})/4\pi$ depends only on the total number of vortices but not on their positions, implying that the free energy and the Gibbs free energy are equivalent for the analysis of the vortex interaction. Though this interaction does not depend on the external magnetic field, the related calculations are significantly simplified by assuming a nonzero

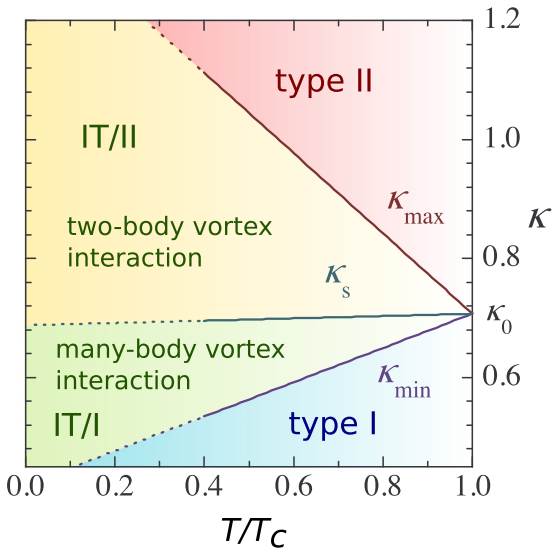

FIG. 2. Phase diagram of the superconductivity types in the (κ, T) plane. The outer and internal boundaries of the IT domain at $T > 0.4$–$0.5T_c$ are given by Eq. (13). At lower temperatures the linear dependence of the boundaries on τ is not applicable (see Ref. [29]); the dashed lines serve as a guide to an eye.

value of H and choosing $H = H_c$ (H_c is the thermodynamic critical field). Finally, we subtract the Gibbs free energy G_M of the uniform Meissner state at $H = H_c$ so that the Gibbs free energy difference $\mathcal{G} = G - G_M$ is analyzed.

We note that the calculations should employ the approach beyond the GL theory. Within the GL theory the IT domain is reduced to the single point $\kappa = \kappa_0$, where the superconducting state at $H = H_c$ is degenerate due to the Bogomolnyi self-duality [39,40]. This degeneracy means that $\mathcal{G} = 0$ for any vortex configuration, i.e., vortices do not interact. However, in the exact (BCS) theory the superconducting state is degenerate only in the limit $T \to T_c$, while at $T < T_c$ the degeneracy is removed due to nonlocal effects. This leads to the formation of a finite IT domain (see Fig. 2) between conventional types I and II in the (κ, T) plane [8,11,29]. Solving the microscopic BCS formalism for an arbitrary multivortex configuration (with arbitrary separations between vortices) is not practical as it requires huge computational efforts.

In this work we employ the extended GL formalism [41–43] that goes to one order beyond the standard GL theory in the expansion of the microscopic equations over $\tau = 1 - T/T_c$. Since we are focused on superconductors with $\kappa \sim \kappa_0$, we also employ the expansion in $\delta\kappa = \kappa - \kappa_0$ retaining its leading contribution [13,29].

Using earlier results for the model of a clean s-wave single-band superconductor with the spherical Fermi surface [29,42] we obtain the Gibbs free-energy difference as

$$\mathcal{G} = \int dV\left[g^{(0)} + g_\kappa^{(1)}\,\delta\kappa + g_\tau^{(1)}\,\tau\right]. \tag{1}$$

Here the GL contribution at $\kappa = \kappa_0$ is given by

$$g^{(0)} = \tfrac{1}{2}(B-1)^2 + |\mathbf{D}\Psi|^2 - |\Psi|^2 + \tfrac{1}{2}|\Psi|^4, \tag{2}$$

where Ψ is the order parameter, $\mathbf{D} = \boldsymbol{\nabla} + \mathbb{i}\mathbf{A}$ is the gauge invariant gradient, and all quantities are scaled using the

characteristic units of the GL theory [see Eq. (15) of Ref. [29]]. The contribution $\propto\delta\kappa$ is also given by the GL theory and reads

$$g_\kappa^{(1)} = -\sqrt{2}B(B-1) - 2\sqrt{2}|\mathbf{D}\Psi|^2. \tag{3}$$

The leading correction in τ follows from the τ expansion of the BCS free energy and is given by

$$\begin{aligned} g_\tau^{(1)} &= (B-1)\left(\frac{1}{2}+c\right) - \frac{1}{2}|\Psi|^2 + 2|\mathbf{D}\Psi|^2 + |\Psi|^4 \\ &+ \mathcal{Q}\left\{|\mathbf{D}^2\Psi|^2 + \frac{1}{3}(\mathrm{rot}\,\mathbf{B}\cdot\mathbf{i}) + B^2|\Psi|^2\right\} \\ &+ \frac{\mathcal{L}}{2}\{8|\Psi|^2|\mathbf{D}\Psi|^2 + [\Psi^2(\mathbf{D}^*\Psi^*)^2 + \mathrm{c.c.}]\} + c\,|\Psi|^6, \end{aligned} \tag{4}$$

with the GL supercurrent density $\mathbf{i} = 2\,\mathrm{Im}[\Psi\mathbf{D}^*\Psi^*]$. The coefficients $c = -0.227$, $\mathcal{L} = -0.454$, and $\mathcal{Q} = -0.817$ in Eq. (4) are material independent for the chosen model [29]. The order parameter and the magnetic field are found from the GL equations

$$\Psi(1-|\Psi|^2) + \mathbf{D}^2\Psi = 0, \quad \mathrm{rot}\mathbf{B} = \mathbf{i}, \tag{5}$$

which can be represented as the two self-duality Bogomolnyi equations [39,40]

$$B = 1 - |\Psi|^2, \quad (\partial_y + \mathbb{i}\partial_x)\Psi = (A_x - \mathbb{i}A_y)\Psi \tag{6}$$

(a solution to this system is also refereed to as the Sarma solution [2]). Using a solution to these equations, one can represent $\mathcal{G}$ (per unit length in the field direction) in the form

$$\mathcal{G} = -\sqrt{2}\mathcal{I}\delta\kappa + (c_\mathcal{J}\mathcal{J} - c_\mathcal{I}\mathcal{I})\tau, \tag{7}$$

with the constants $c_\mathcal{I} = 0.407$ and $c_\mathcal{J} = 0.681$ and

$$\mathcal{I} = \int dV|\Psi|^2(1-|\Psi|^2), \quad \mathcal{J} = \int dV|\Psi|^4(1-|\Psi|^2). \tag{8}$$

The GL contribution at $\kappa = \kappa_0$ disappears in Eq. (7), reflecting the Bogomolnyi degeneracy, so that the final result contains only the terms $\propto\delta\kappa,\tau$. It is of importance that $\mathcal{G}$ defined by Eqs. (7) and (8) depends only on a solution to Eq. (5) [or Eq. (6)], demonstrating that properties of the vortex matter in the IT domain are fully determined by the Bogomolnyi self-duality.

We note that a similar expression for $\mathcal{G}$ can be obtained for multiband superconductors provided that the system does not have a special symmetry in addition to $U(1)$ [29]. In this case the coefficients $c_{\mathcal{I},\mathcal{J}}$ become material dependent and have contributions of all bands as well as of the interband coupling. This leads to considerable quantitative changes while the qualitative picture remains the same [29].

Solutions to the Bogomolnyi equations are conveniently found by introducing a new scalar field as $A_x = -\partial_y\phi$, $A_y = \partial_x\phi$, so that $B = \Delta\phi$, with $\Delta = \partial_x^2 + \partial_y^2$. Using the substitution $\Psi = \exp(-\phi)\Phi$, we recast Eq. (6) in the form

$$\Delta\phi = 1 - e^{-2\phi}|\Phi|^2, \quad (\partial_y + \mathbb{i}\partial_x)\Phi = 0. \tag{9}$$

The solution that describes N vortices with the centers at $\mathbf{r}_i$ is obtained as follows. We first find $\Psi_1(\mathbf{r})$ that describes an isolated Abrikosov vortex with the center at $\mathbf{r} = 0$. Then we represent the N-vortex solution in the form

$$\Psi(\mathbf{r}) = e^{-\theta}\prod_{i=1}^{N}\Psi_i, \quad \Psi_i = \Psi_1(\mathbf{r}-\mathbf{r}_i). \tag{10}$$

Substituting this into Eq. (9) and taking into account that Ψ_1 is also a solution of the Bogomolnyi equations, we obtain

$$\Delta\theta = 1 + \sum_i(|\Psi_i|^2 - 1) - e^{-2\theta}\prod_i|\Psi_i|^2. \tag{11}$$

Solving this equation and substituting the obtained Ψ into Eqs. (7) and (8), we find the Gibbs free energy difference $\mathcal{G}$ for the N-vortex cluster in question and then extract the corresponding interaction energy (interaction potential) by subtracting the energies of N isolated vortices. The interaction potential (per vortex) is given by

$$\mathcal{G}_\mathrm{int} = \mathcal{G}/N - \mathcal{G}_1, \tag{12}$$

where the Gibbs free energy difference for an isolated vortex $\mathcal{G}_1$ is found by using the single vortex solution.

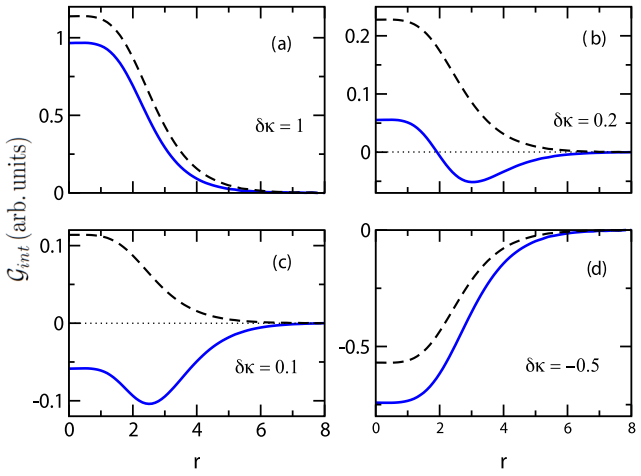

FIG. 3. Solid (blue) curve: the interaction potential $\mathcal{G}_\mathrm{int}$ (per vortex and per unit length) for the 2-vortex configuration versus the distance r between vortices. Panels (a), (b), (c), and (d) correspond to $\delta\kappa = 1$ (type II), 0.2 (IT/II), 0.1 (IT/II), and -0.5 (type I). The dashed (black) curve represents $\mathcal{G}_\mathrm{int}$ for the same configuration but calculated from the GL theory.

III. RESULTS

Since the focus of this study is the properties of superconductors in the IT domain, we first specify its boundaries recalling earlier results [7,29,44]. Its lower boundary $\kappa_\mathrm{min}(T)$ is obtained from the condition $H_c = H_{c2}$ (H_{c2} is the upper critical field), which determines the appearance of the mixed state, while the upper boundary $\kappa_\mathrm{max}(T)$ marks the onset of the long-range attraction between vortices. Subdomains IT/I and IT/II are separated by $\kappa_s(T)$ determined by the condition of a vanishing surface energy of the flat superconducting-normal domain wall. Using the extended GL formalism for a clean s-wave single-band superconductor with a spherical Fermi

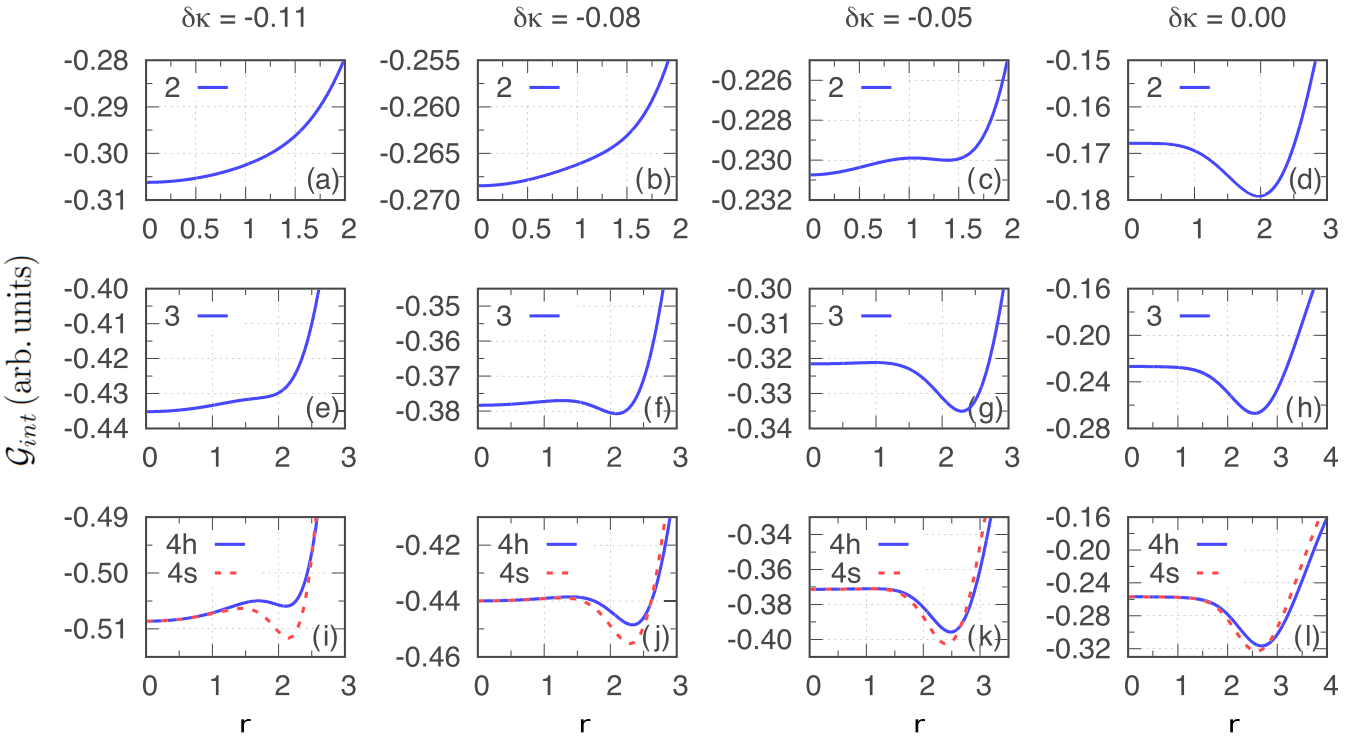

FIG. 4. Vortex interaction potential $\mathcal{G}_{\rm int}$ as a function of the distance r between neighboring vortices, calculated for the N-vortex configurations ($N = 2,3,4$), shown in Fig. 1, and for $\delta\kappa = -0.11, -0.08, -0.05$, that correspond to the IT/I subdomain, and $\delta\kappa = 0$, that is in the vicinity of the boundary between the IT/I and IT/II subdomains. The units are the same as in Fig. 3.

surface, we obtain [29]

$$\kappa_{\rm min} = \kappa_0 - 0.41\tau, \quad \kappa_{\rm max} = \kappa_0 + 0.95\tau, \kappa_{\rm s} = \kappa_0 - 0.03\tau. \tag{13}$$

In Fig. 2, a simplified phase diagram of the superconductivity types is shown in the (κ, T) plane, with the outer and internal boundaries of the IT domain determined by Eq. (13) (a more detailed diagram can be found in Ref. [29]). We note that, although the linear τ dependence of $\kappa_{\rm min}$, $\kappa_{\rm max}$, and $\kappa_{\rm s}$ is obtained in the vicinity of T_c, it has been demonstrated [29] that the applicability of Eq. (13) extends down to temperatures 0.4–0.5T_c.

We note that due to the linear dependence of the energy $\mathcal{G}_{\rm int}$ in Eq. (12) on both τ and $\delta\kappa$, the characteristic boundaries that control changes in the interaction energy are linear functions of τ. Thus it is possible to choose $\tau = 1$ for convenience; results for $\tau < 1$ are simply obtained by the corresponding rescaling.

A. 2-vortex cluster

We first consider the interaction potential between two vortices, which is plotted in Fig. 3 as a function of the intervortex distance r (in units of $\sqrt{2}\lambda$, with λ the magnetic penetration depth). Panels (a) and (d) represent, respectively, type-II ($\delta\kappa = 1$) and type I ($\delta\kappa = -0.5$) superconductivity; panels (b) and (c) are calculated for the IT/II regime ($\delta\kappa = 0.2, 0.1$). For type II superconductors the interaction potential is a monotonically decreasing function [see Fig. 3(a)] so that vortices are repulsive at all distances. For type I materials the potential is a monotonically increasing function [see Fig. 3(d)], vortices attract each other, and the 2-vortex configuration is unstable.

In the IT domain the interaction potential is no longer monotonic, as illustrated in Figs. 3(b) and 3(c) for $\delta\kappa = 0.2$ and 0.1, respectively. In both cases vortices are repulsive at short and attractive at large intervortex distances, with the potential minimum achieved at some finite distance $r_{\rm min}$. This agrees with the earlier results and is in line with the type II/1,2 picture. For comparison, the dashed curve in each panel of Fig. 3 represents the corresponding GL result given by the first term $\propto\delta\kappa$ in Eq. (7).

Figures 4(a)–4(d) show the two-vortex interaction potential calculated at $\delta\kappa = 0$ (near the boundary between the IT/I and IT/II subdomains) and at $\delta\kappa = -0.11, -0.08, -0.05$ (all in the IT/I subdomain). The results confirm the trend, seen in Fig. 2, that the two-vortex interaction becomes more attractive at smaller $\delta\kappa$. The transformation from the nonmonotonic dependence to the full attraction takes two steps: the minimum at $r_{\rm min}$ (1) becomes local and (2) disappears. It is important that the full-attraction regime is reached before type I is achieved (i.e., before crossing the lower boundary of the intertype domain): Fig. 4(b) shows an attractive potential for $\delta\kappa = -0.08$, which is still far from the lower boundary of the IT interval at $\tau = 1$, i.e., $\delta\kappa_{\rm min} = \kappa_{\rm min} - \kappa_0 = -0.41$.

B. 3- and 4-vortex clusters

We now turn to the 3- and 4-vortex clusters, where the interaction potential contains many-body contributions. The interaction potential for the 3-vortex cluster is illustrated in

Figs. 4(e)–4(h). One sees that, in the vicinity of the boundary between the IT/I and IT/II subdomains, at $\delta\kappa = 0$, the 2- and 3-vortex interaction potentials are qualitatively similar [cf. Figs. 4(d) and 4(h)]. In fact, this similarity holds for any $\delta\kappa > 0$, i.e., for the IT/II and type II regimes. It also extends to the case of the 4-vortex clusters [cf. Fig. 4(l)]. This leads us to the conclusion that in the IT/II subdomain the many-body contributions do not lead to qualitative changes in the total vortex interaction. Furthermore, for type II superconductors the many-body corrections to the vortex interaction are negligible, as expected. This is the reason why only results for $\delta\kappa < 0$ are given in Fig. 4.

On the contrary, in the IT/I subdomain the situation changes dramatically. For example, for $\delta\kappa = -0.05$ the global minimum of the 3-vortex potential is found at $r_{\min} \simeq 2.3$ [see Fig. 4(g)]. However, for the two-vortex configuration the global minimum is at $r = 0$ [see Fig. 4(c)]. At $\delta\kappa = -0.08$ the global minimum of the 3-vortex potential slightly shifts to $r \simeq 2.2$ [see Fig. 4(f)] while the 2-vortex interaction is already fully attractive [see Fig. 4(b)]. The interaction potentials for 2- and 3-vortex clusters become both fully attractive only at $\delta\kappa = -0.11$ [Figs. 4(a) and 4(e)]. This qualitative difference between the interaction in the 2- and 3-vortex clusters indicates an increased role of the many-body interactions. We stress that in some parameter range the 3-vortex configuration is stable while the 2-vortex cluster collapses.

The results for the 4-vortex configurations are shown in Figs. 4(i)–4(k) and further confirm the increased role of the many-body interactions in superconductors closer to type I. At $\delta\kappa = -0.05$ the potentials for both h and s clusters are qualitatively similar to that of the 3-vortex configuration [see Figs. 4(k) and 4(g)]. However, at $\delta\kappa = -0.08$ the quantitative difference between the 3- and 4-vortex interaction potentials is already notable [see Figs. 4(f) and 4(j)]. Finally, at $\delta\kappa = -0.11$ the 3- and 4-vortex potentials become qualitatively different: the interaction is fully repulsive for the 3-vortex cluster [see Fig. 4(e)] while both potentials for the 4-vortex case are still nonmonotonic [see Fig. 4(i)]. Furthermore, at $\delta\kappa = -0.11$ the interactions in the h and s configurations of the 4-vortex cluster become significantly different: in the h configuration the absolute minimum of the potential is found at $r = 0$ but the s cluster still favors a finite distance between vortices $r_{\min} \simeq 2.1$. One sees that there is an interval of $\delta\kappa$, where 4-vortex clusters are stable due to four-body interactions while 3- and 2-vortex configurations collapse.

Finally, in order to illustrate relations between the vortex interaction and the IT subdomains we superimpose the results for the vortex interaction on the phase diagram given in Fig. 2.

IV. CONCLUSIONS

Our analysis of the vortex interactions in IT superconductors has revealed that contrary to the standard type II/1,2 picture, vortex-matter configurations are not determined by the 2-vortex interactions in the entire IT domain. The calculations have demonstrated qualitative differences between the IT/I and IT/II subdomains. In the IT/II subdomain the vortex interaction potential has the two-body character and a nonmonotonic spatial dependence with long-range attraction and short-range repulsion, which agrees with the concept of type II/1,2 superconductivity. However, in the IT/I subdomain many-body interactions play a crucial role, and the spatial dependence of a many-body potential differs qualitatively from that of the two-body one. For example, many-body interactions in large vortex clusters remain repulsive at short distances even when the two-body interaction is fully attractive. An important consequence is that many-body interactions in the IT/I subdomain stabilize large vortex clusters.

This observation supports the general conclusion that a superconductor in the IT/I regime can develop a very peculiar vortex matter, where vortices would not exist without many-body interactions.

Finally, we note that the universality of the EGL formalism for systems with an arbitrary number of bands ensures that qualitatively similar conclusions can be expected for multiband superconductors.

ACKNOWLEDGMENTS

This work was supported by the Brazilian agencies CAPES (Grants No. 223038.003145/2011-00 and No. 400510/2014-6), CNPq (Grant No. 309374/2016-2), and FACEPE (Grant No. APQ-0936-1.05/15). A.V. is grateful to the Physics Department of the Federal University of Pernambuco, Recife, Brazil, for hospitality.

[1] E. M. Lifshitz and L. P. Pitaevskii, *Statistical Physics, Part 2, Landau and Lifshitz Course of Theoretical Physics, Volume 9* (Pergamon, Oxford, 1980).
[2] P. G. de Gennes, *Superconductivity of Metals and Alloys* (Benjamin, New York, 1966).
[3] J. B. Ketterson and S. N. Song, *Superconductivity* (Cambridge University Press, Cambridge, UK, 1999).
[4] U. Krägeloh, Phys. Lett. A **28**, 657 (1969).
[5] U. Essmann, Physica **55**, 83 (1971).
[6] D. R. Aston, L. W. Dubeck, and F. Rothwarf, Phys. Rev. B **3**, 2231 (1971).
[7] A. E. Jacobs, Phys. Rev. Lett. **26**, 629 (1971).
[8] J. Auer and H. Ullmaier, Phys. Rev. B **7**, 136 (1973).
[9] U. Klein, J. Low Temp. Phys. **69**, 1 (1987).
[10] U. Klein, J. Rammer, and W. Pesch, J. Low Temp. Phys. **66**, 55 (1987).
[11] H. W. Weber, E. Seidl, M. Botlo, C. Laa, E. Mayerhofer, F. M Sauerzopf, R. M. Schalk, and H. P. Wiesingerh, Physica C **161**, 272 (1989).
[12] E. H. Brandt, Rep. Prog. Phys. **58**, 1465 (1995).
[13] I. Luk'yanchuk, Phys. Rev. B **63**, 174504 (2001).
[14] M. Laver, E. M. Forgan, S. P. Brown, D. Charalambous, D. Fort, C. Bowell, S. Ramos, R. J. Lycett, D. K. Christen, J. Kohlbrecher, C. D. Dewhurst, and R. Cubitt, Phys. Rev. Lett. **96**, 167002 (2006).

[15] M. Laver, C. J. Bowell, E. M. Forgan, A. B. Abrahamsen, D. Fort, C. D. Dewhurst, S. Mühlbauer, D. K. Christen, J. Kohlbrecher, R. Cubitt, and S. Ramos, Phys. Rev. B **79**, 014518 (2009).
[16] S. Mühlbauer, C. Pfleiderer, P. Böni, M. Laver, E. M. Forgan, D. Fort, U. Keiderling, and G. Behr, Phys. Rev. Lett. **102**, 136408 (2009).
[17] E. H. Brandt and M. P. Das, J. Supercond. Nov. Magn. **24**, 57 (2011).
[18] A. Pautrat and A. Brûlet, J. Phys.: Condens. Matter **26**, 232201 (2014).
[19] Y. Wang, R. Lortz, Y. Paderno, V. Filippov, S. Abe, U. Tutsch, and A. Junod, Phys. Rev. B **72**, 024548 (2005).
[20] J.-Y. Ge, J. Gutierrez, A. Lyashchenko, V. Filipov, J. Li, and V. V. Moshchalkov, Phys. Rev. B **90**, 184511 (2014).
[21] J.-Y. Ge, V. N. Gladilin, N. E. Sluchanko, A. Lyashenko, V. B. Filipov, J. O. Indekeu, and V. V. Moshchalkov, New J. Phys. **19**, 093020 (2017).
[22] M. Tinkham, Phys. Rev. **129**, 2413 (1963).
[23] J. Pearl, Appl. Phys. Lett. **5**, 65 (1964).
[24] K. Maki, Ann. Phys. (NY) **34**, 363 (1965).
[25] G. Lasher, Phys. Rev. **154**, 345 (1966).
[26] G. J. Dolan and J. Silcox, Phys. Rev. Lett. **30**, 603 (1973).
[27] S. Hasegawa, T. Matsuda, J. Endo, N. Osakabe, M. Igarashi, T. Kobayashi, M. Naito, A. Tonomura, and R. Aoki, Phys. Rev. B **43**, 7631 (1991).
[28] K. O. Moura, K. R. Pirota, F. Béron, C. B. R. Jesus, P. F. S. Rosa, D. Tobia, P. G. Pagliuso, and O. F. de Lima, Type-II Superconductivity in Arrays of Nanostructured β-Gallium, Abstract Book for 16th International Workshop on Vortex Matter in Superconductors, Natal, Brazil, 2017 (unpublished).
[29] A. Vagov, A. A. Shanenko, M. V. Milošević, V. M. Axt, V. M. Vinokur, J. A. Aguiar, and F. M. Peeters, Phys. Rev. B **93**, 174503 (2016).
[30] S. Wolf, A. Vagov, A. A. Shanenko, V. M. Axt, A. Perali, and J. A. Aguiar, Phys. Rev. B **95**, 094521 (2017).
[31] Y. Lubashevsky, E. Lahoud, K. Chashka, D. Podolsky, and A. Kanigel, Nat. Phys. **8**, 309 (2012).
[32] S. Kasahara, T. Watashige, T. Hanaguri, Y. Kohsaka, T. Yamashita, Y. Shimoyama, Y. Mizukami, R. Endo, H. Ikeda, K. Aoyama, T. Terashima, S. Uji, T. Wolf, H. von Löhneysenn, T. Shibauchi, and Y. Matsuda, Proc. Natl. Acad. Sci. USA **111**, 16309 (2014).
[33] K. Okazaki, Y. Ito, Y. Ota, Y. Kotani, T. Shimojima, T. Kiss, S. Watanabe, C.-T. Chen, S. Niitaka, T. Hanaguri, H. Takagi, A. Chainani, and S. Shin, Sci. Rep. **4**, 4109 (2014).
[34] A. Chaves, F. M. Peeters, G. A. Farias, and M. V. Milošević, Phys. Rev. B **83**, 054516 (2011).
[35] J. Carlström, J. Garaud, and E. Babaev, Phys. Rev. B **84**, 134515 (2011).
[36] L. Komendová, M. V. Milošević, and F. M. Peeters, Phys. Rev. B **88**, 094515 (2013).
[37] R. M. da Silva, M. V. Milošević, A. A. Shanenko, F. M. Peeters, and J. Albino Aguiar, Sci. Rep. **5**, 16515 (2015).
[38] W. Y. Córdoba-Camacho, R. M. da Silva, A. Vagov, A. A. Shanenko, and J. A. Aguiar, Phys. Rev. B **94**, 054511 (2016).
[39] E. B. Bogomolnyi and A. I. Vainstein, Sov. J. Nucl. Phys. **23**, 588 (1976).
[40] E. B. Bogomolnyi, Sov. J. Nucl. Phys. **24**, 449 (1976).
[41] A. A. Shanenko, M. V. Milošević, F. M. Peeters, and A. V. Vagov, Phys. Rev. Lett. **106**, 047005 (2011).
[42] A. V. Vagov, A. A. Shanenko, M. V. Milošević, V. M. Axt, and F. M. Peeters, Phys. Rev. B **85**, 014502 (2012).
[43] A. Vagov, A. A. Shanenko, M. V. Milošević, V. M. Axt, and F. M. Peeters, Phys. Rev. B **86**, 144514 (2012).
[44] A. E. Jacobs, Phys. Rev. B **4**, 3016 (1971); **4**, 3022 (1971); **4**, 3029 (1971).